IEEE Photonics Journal
An IEEE Photonics Society Publication

Open Access

Advantages of AlGaN-Based 310-nm UV Light-Emitting Diodes With Al Content Graded AlGaN Electron Blocking Layers

Volume 5, Number 4, August 2013

Yang Li
Shengchang Chen
Wu Tian
Zhihao Wu
Yanyan Fang
Jiangnan Dai
Changqing Chen

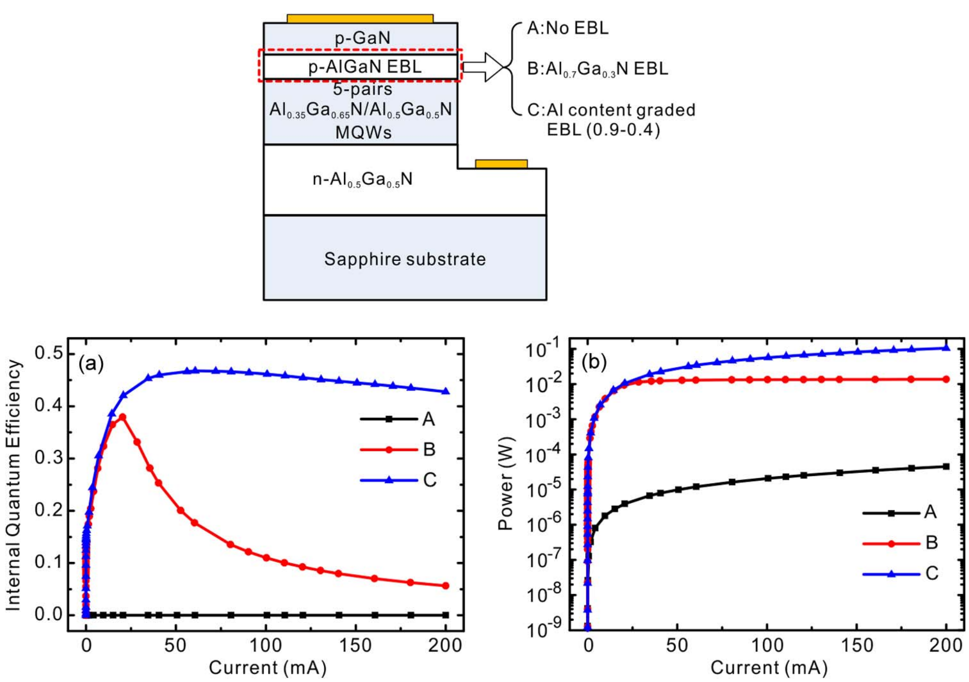

DOI: 10.1109/JPHOT.2013.2271718
1943-0655/$31.00

Advantages of AlGaN-Based 310-nm UV Light-Emitting Diodes With Al Content Graded AlGaN Electron Blocking Layers

Yang Li, Shengchang Chen, Wu Tian, Zhihao Wu, Yanyan Fang, Jiangnan Dai, and Changqing Chen

Wuhan National Laboratory for Optoelectronics, School of Optical and Electronic Information, Huazhong University of Science and Technology, Wuhan 430074, China

DOI: 10.1109/JPHOT.2013.2271718

Manuscript received May 27, 2013; revised June 16, 2013; accepted June 17, 2013. Date of publication July 3, 2013; date of current version July 11, 2013. This work was supported in part by the National Basic Research Program of China (973 Program) under Grant 2012CB619302 and in part by the National Natural Science Foundation of China under Grants 10990103, 51002058, and 11104150.
Corresponding author: Z. H. Wu (e-mail: zhihao.wu@mail.hust.edu.cn).

Abstract: In order to improve the performance of deep ultraviolet light-emitting diodes (UV LEDs), the effects of different electron blocking layers (EBLs) on the performance of $Al_xGa_{1-x}N$-based deep UV LEDs at 310 nm have been studied through a numerical simulation. The simulation results show that the adoption of EBLs is critical to improve the device performance. In comparison with a conventional structure using EBL with constant Al composition (0.7), the device structure with an Al-content graded $Al_xGa_{1-x}N$ (from 0.9 to 0.4 in the growth direction) EBL possesses numerous advantages such as lower working voltage, higher internal quantum efficiency, and less efficiency droop under high-current injection. By detailedly analyzing the profiles of energy band diagrams, distributions of carrier concentration, and electron current density, the advantages of Al-content graded $Al_xGa_{1-x}N$ EBL are attributed to the resulting lower resistivity, higher barrier for electron leakage, and simultaneously reduced barrier for hole injection compared with the conventional EBL with constant Al composition.

Index Terms: III-Nitride, graded AlGaN electron blocking layer, ultraviolet light-emitting diodes.

1. Introduction

Recently, the development of deep ultraviolet light-emitting diodes (UV LEDs) based on high Al content $Al_xGa_{1-x}N$ materials has attracted considerable attention because of their wide range of potential applications such as air and water purification, surface disinfection, UV curing, and medical phototherapy. Despite their tremendous opportunities, $Al_xGa_{1-x}N$ based deep UV LEDs still suffer from relatively low external quantum efficiency (EQE) and emission power [1]. The EQEs of the reported $Al_xGa_{1-x}N$ based deep UV LEDs with emission wavelengths from 280 to 350 nm are typically less than 10%, which are about one order of magnitude lower than those of LEDs in the near UV and visible spectral range based on $In_xGa_{1-x}N$ [2]–[5]. There are multiple causes responsible for the low efficiencies of AlGaN based deep UV LEDs. First of all, the high dislocation density in high Al content AlGaN materials grown on sapphire substrates leads to severe nonradiative recombination [6], [7]. Second, the strong spontaneous and piezoelectric polarization charges induced at the interface of the active layers make the band diagrams of quantum wells (QWs) tilted and result in reduced overlap of electron and hole wavefunctions, which further deteriorates the radiative recombination rate [8], [9]. Furthermore, the strong electron leakage due to the large imbalance in electron and hole injection in deep UV LEDs is regarded as an important factor causing the low internal quantum efficiency (IQE) [10]. For the first issue, low defect AlN bulk substrates and migration enhanced growth of AlN templates on sapphire substrates have been adopted to reduce the dislocation density in $Al_xGa_{1-x}N$ materials [7], [11]. While for the latter two issues, energy band engineering method would be a good solution. Recently, various energy band engineering methods have been widely used to improve the peak efficiency and to reduce the efficiency droop in III-nitrides based LEDs. For instance, staggered QWs [12]–[17], InGaN/GaNAs or InGaN/GaNSb/GaN type-II QWs [18]–[20], InGaN QWs with delta layer [21]–[23], single quantum well with thin $Al_{0.83}In_{0.17}N$ barriers [24] and polarization matched GaInN/AlGaInN QWs [25] were designed to enhance the spontaneous emission rate in InGaN QWs by increasing the electron-hole wavefunction overlap. Wide double heterostructure (DH) active regions were used to reduce Auger recombination [26], and thus reducing the efficiency droop. In case of AlGaN based UV LEDs, thin QWs are used in the active region to relieve the polarization effect and enhance the radiative recombination of carriers [27]. Also, an $Al_xGa_{1-x}N$ layer of higher Al content than that in MQWs or AlN layer is inserted between the active region and p-type hole-injection layer with the hope that the wider bandgap material layer would act as an electron-blocking layer (EBL) to suppress the escape of the electrons out of the active region into the p-type hole injection layer [10], [28]–[32]. At the same time, progress have been accomplished in the past few years on the understanding of the physics of gain media and device physics of mid and deep UV LEDs based on high Al content AlGaN QWs [33]–[38]. The identification of large TM-polarized gain in high Al-content AlGaN QW [33], [34] and the use of delta-based QW active regions [35]–[38] have been reported. All these results show the great potentials of band engineering in improving the device characteristics of UV LEDs.

Although constant Al content EBLs have already been commonly used in UV LED structures, the related mechanisms have not been completely understood yet. Very recently, the sensitivity of electron leakage to the design parameters of 1 nm AlN EBL with composition graded interfaces has been studied in Ref. [32], which shows that the electron blocking effect is extremely sensitive not only to the EBL material composition but also to the conduction band offset and to the net polarization. However, the detailed structure and its effects on device performances for the composition graded interfaces of the 1 nm AlN EBL were not elaborated in Ref. [32]. In addition, it is still unclear whether the ultrathin 1 nm AlN EBL has advantages over the more conventional AlGaN EBLs with several tens of nanometers. In this paper, specific designs of $Al_xGa_{1-x}N$ EBLs with conventional thickness for 310 nm emitting UV LED are numerically evaluated in terms of device performances such as working voltage, internal quantum efficiency and efficiency droop. Three device structures are investigated by the APSYS (Advance Physical Model of Semiconductor Devices) simulation program. The first one is the control structure without EBL. The second one is the structure with an $Al_{0.7}Ga_{0.3}N$ EBL, and the third structure uses an Al content graded $Al_xGa_{1-x}N$ (from 0.9 to 0.4 in the growth direction) layer as the EBL. Our simulation results show that the device structure without EBL has the lowest working voltage, but its IQE is extremely low. The adoption of the $Al_{0.7}Ga_{0.3}N$ EBL can greatly upgrade the IQE, but results in higher working voltage. Compared to the $Al_{0.7}Ga_{0.3}N$ EBL, the adoption of Al content graded $Al_xGa_{1-x}N$ EBL cannot only greatly reduce the working voltage, but also can remarkably increase the IQE, and alleviate the efficiency droop effect at large bias current.

2. Device Structure and Simulation Parameters

The properties of the LEDs with different EBLs were investigated numerically with the APSYS (Advanced Physical Model of Semiconductor Devices) simulation program, which was developed by the Crosslight Software Inc. APSYS is capable at solving the Poisson's equation, current continuity equations, carrier transport equations, quantum mechanical wave equation and photon rate equation related to LED physic properties.

Fig. 1 shows the structures of the deep UV LEDs under investigation. The control UV-LED used as reference is designed to be grown on a c-sapphire substrate with a 3-μm-thick Si-doped

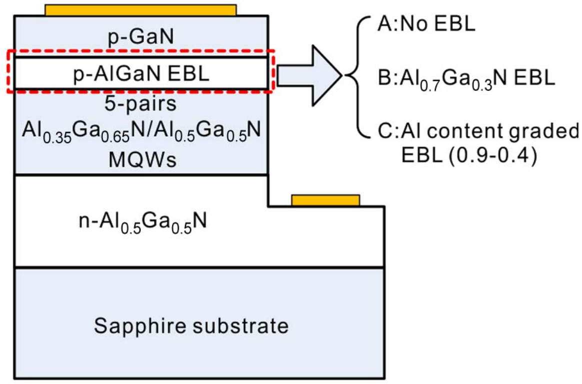

Fig. 1. Vertical cross section of the simulated UV LED structure with lateral injection geometry.

$Al_{0.5}Ga_{0.5}N$ layer (n-doping $= 2 \times 10^{18}$ cm^{-3}). The active region consists of five 3-nm-thick $Al_{0.35}Ga_{0.65}N$ wells separated by six 10-nm-thick Si-doped $Al_{0.5}Ga_{0.5}N$ barriers (n-doping $= 5 \times 10^{17}$ cm^{-3}). The wells are set to be undoped. Since in practice p-type high Al content $Al_xGa_{1-x}N$ layer is difficulty to achieve, a 100-nm-thick p-type GaN (p-doping $= 1 \times 10^{18}$ cm^{-3}) is employed on top of the active region for hole injection and making contacts. The 100-nm thickness of p-GaN is mainly chosen for a good current spreading and for making good contact with p-electrode in reality. The relatively large thickness of this layer will certainly absorb a large portion of the UV light emitted upwards, but it does not matter too much considering the fact that the p-electrode materials like Ni/Au and solder materials for flip-chip bonding like Au/Sn will absorb most of UV light emitted upwards if not all. The control structure without EBL is named as sample A. In order to explore the influence of EBLs on the performance of deep UV LEDs, we designed another two structures with 10-nm-thick p-$Al_xGa_{1-x}N$ EBLs inserted between the active region and p-GaN. One of them (denoted as sample B) contains p-$Al_{0.7}Ga_{0.3}N$ EBL (p-doping $= 2 \times 10^{17}$ cm^{-3}), while the other structure (denoted as sample C) incorporates an Al content graded p-$Al_xGa_{1-x}N$ EBL, in which the Al content is linearly graded from 0.9 to 0.4 in the growth direction. The device geometry is designed to be a square shape of 300 μm $\times$ 300 μm.

The energy bandgap of $Al_xGa_{1-x}N$ ternary alloy at room temperature can be expressed as

$$E_g(Al_xGa_{1-x}N) = xE_g(AlN) + (1-x)E_g(GaN) - 0.7x(1-x) \tag{1}$$

where the values of bandgap at room temperature under unstrained condition are 6.138 and 3.435 eV for AlN and GaN, respectively [39]. Both the band offset ratios of AlGaN/AlGaN and AlGaN/GaN are set to be 0.5/0.5 according to the report of Piprek *et al.* [40]. The polarization effect of $Al_xGa_{1-x}N$ alloy with wurtzite structures is considered using the model of Fiorentini *et al.* [41] with 50% of the polarization charges compensated by defects and interface charges. The Caughey-Thomas approximation [42] is introduced to depict the mobility as a function of carrier density

$$\mu(N) = \mu_{min} + \frac{\mu_{max} - \mu_{min}}{1 + (N/N_{ref})^{\alpha}} \tag{2}$$

where μ_{min}, μ_{max}, N_{ref}, and α are the fitting parameters of the Caughey-Thomas model. Other parameters used in the simulation are listed as follows: the operating temperature is set at 300 K, nonradiative carrier lifetime is set to be 5 ns and internal absorption within the LED device is assumed to be 1000 m^{-1} here. We assume the extraction efficiency of light out of the substrate bottom to be 30%, considering that light emitted toward p-side (50% of total light emission) is completely lost, and a 60% of light emitted toward sapphire is extracted out of the substrate bottom. Detailed material parameters of semiconductors used in this simulation can be found in [39].

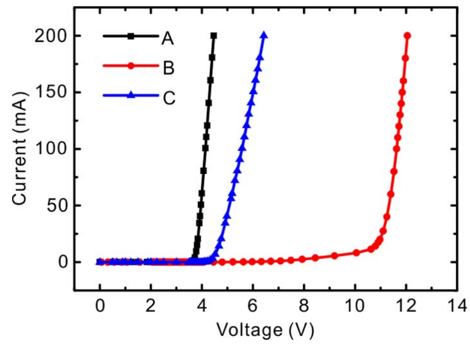

Fig. 2. Simulated *I–V* performance curves of three samples.

3. Results and Discussion

The simulated current-voltage (*I–V*) curves of the three samples are plotted in Fig. 2. The turn-on voltage of sample A is 3.7 V. While for sample B, the adoption of p-$Al_{0.7}Ga_{0.3}N$ EBL increases the turn-on voltage remarkably to about 10.7 V, which should be attributed to the high resistance nature of p-$Al_{0.7}Ga_{0.3}N$ EBL. Due to the high activation energies of Mg in high Al content $Al_xGa_{1-x}N$ materials, the hole concentration is very low, leading to a large resistivity. On the other hand, the turn-on voltage of sample C is found to be 4.4 V, only slightly larger than that of sample A, which indicates that the Al content graded p-$Al_xGa_{1-x}N$ EBL in sample C has larger conductivity than the EBL in sample B.

Fig. 3 shows the energy band diagrams and quasi-Fermi levels of deep UV LEDs with different EBLs at injection current of 200 mA. As shown in Fig. 3(a), there is no energy barrier at the top side of the MQWs in sample A since no EBL was adopted. Due to the rapid drop of the conduction band energy from the last barrier to the p-GaN layer, electrons can easily overflow to the p-GaN layer because of the higher density and mobility of electrons than holes. Thus electron leakage will be a serious problem in sample A. For the band diagram of sample B with p-$Al_{0.7}Ga_{0.3}N$ EBL shown in Fig. 3(b), we first notice that severe band tilting with a total potential drop of 6.6 eV occurs in the p-$Al_{0.7}Ga_{0.3}N$ EBL. The large potential drop is essential to generate 200 mA current in the high resistance p-$Al_{0.7}Ga_{0.3}N$ EBL. In Fig. 3(c), we can clearly see that a triangle potential barrier of 207 meV height for electrons is formed between the last barrier and the p-$Al_{0.7}Ga_{0.3}N$ EBL, which can reduce the electron leakage. However, due to the severe band tilting in p-$Al_{0.7}Ga_{0.3}N$ EBL, the barrier becomes so thin that electrons might easily tunnel through it. In addition, due to the large difference in polarizations between the last $Al_{0.5}Ga_{0.5}N$ barrier and the p-$Al_{0.7}Ga_{0.3}N$ EBL, a high density of positive polarization charges exist at their interface, which attracts electrons from the n-type side and repel holes from the p-type side. Therefore, the band of the last $Al_{0.5}Ga_{0.5}N$ barrier severely bends downward, facilitating the leakage of electrons from the last quantum well. At the interface between the p-$Al_{0.7}Ga_{0.3}N$ EBL and the p-type GaN layer, a barrier of 314 meV height [see Fig. 3(d)] for hole transport is present, which will significantly lower the probability of hole injection into MQW regions. In contrast, as shown in Fig. 3(e), when Al content graded EBL is adopted as in sample C, the barrier height for electrons is increased to 449 meV, which means much enhanced electron blocking effect in sample C as compared to sample B. The higher electron barrier should be mainly due to the larger band offset of $Al_{0.5}Ga_{0.5}N/Al_{0.9}Ga_{0.1}N$ at the interface of the last $Al_{0.5}Ga_{0.5}N$ barrier and the Al content graded EBL. The band tilting in the Al content graded EBL is much alleviated as compared to sample B, which is helpful for blocking the electron leakage. The Al content graded EBL has a high density of holes as will be shown later. Its high conductivity will reduce the voltage drop across this layer. The smaller band offset of $Al_{0.4}Ga_{0.6}N$/GaN at the interface of the graded EBL and the p-type GaN layer in sample C reduces the effective potential height for holes from 314 meV in sample B to 249 meV. Accordingly, the use of Al content graded EBL can

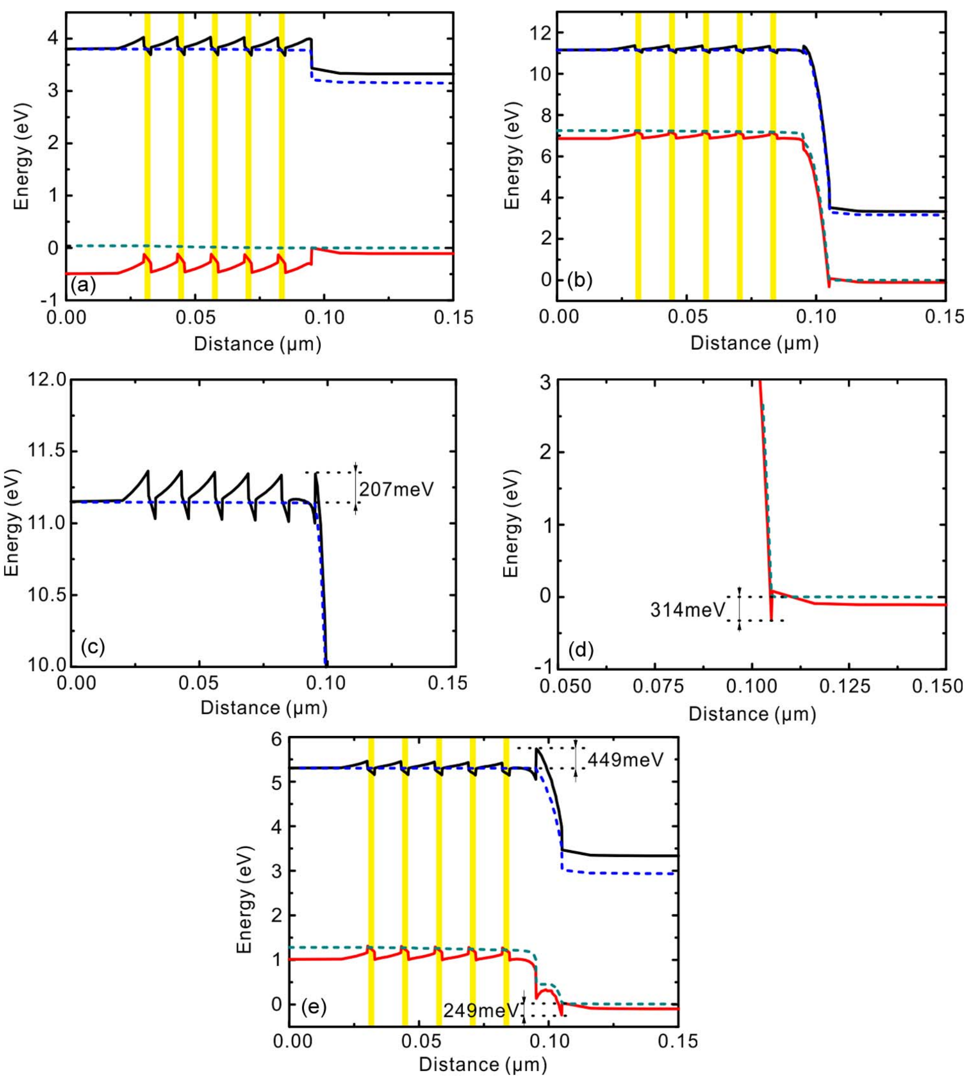

Fig. 3. Energy band diagrams of (a) sample A, (b) sample B and (e) sample C at bias current of 200 mA and the enlarged drawings of the (c) conduction band and (d) valance band of sample B.

effectively enhance the electron confinement and reduce the barrier for holes to inject into active region at the same time.

Fig. 4 shows the profiles of carrier concentration across the active region at the bias current of 200 mA for the three samples with different EBLs. As shown in Fig. 4(a), the electron concentrations of the first three quantum wells in samples A and B are almost the same, about 4.0×10^{18} cm^{-3}, while those in the last two wells are noticeably higher in sample B than in sample A. In addition, going from the last barrier to the p-type GaN layer, the electron concentration of sample B drops rapidly from 3.3×10^{19} cm^{-3} to 4.9×10^{14} cm^{-3}, indicating that the p-$Al_{0.7}Ga_{0.3}N$ EBL is helpful to reduce electron leakage into the p-GaN. Compared with sample A and sample B, the electron concentrations in all MQWs of sample C are much higher, and that in the p-type layer decreases obviously. The much lower electron concentration in p-type layer is the proof of enhanced electron blocking effect in sample C resulted from the highest barrier for electrons. On the other hand, the distribution of hole concentration in MQWs also varies with the EBL layers as shown in Fig. 4(b). The hole concentrations in MQWs of sample A are very low compared with sample B and C. Considering the much lower density and mobility of holes compared with electrons, electrons in

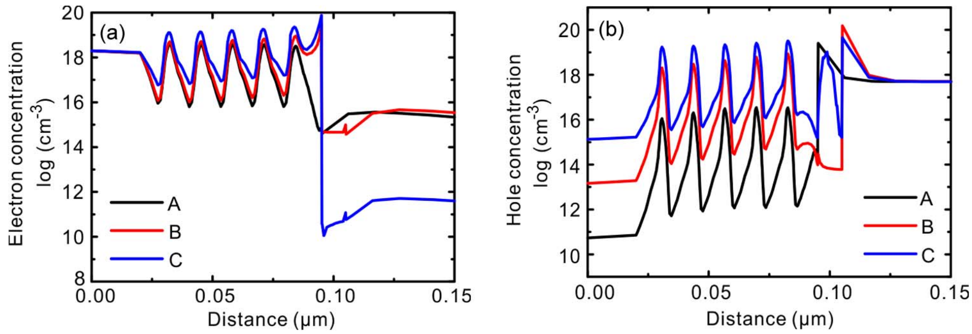

Fig. 4. Distribution of (a) electron concentration and (b) hole concentration of sample A, B and C at bias current of 200 mA.

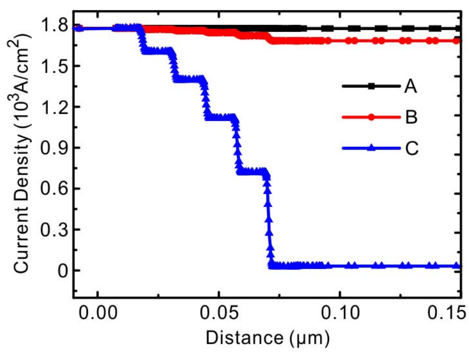

Fig. 5. Distributions of electron current density near the active regions of sample A, B and C at bias current of 200 mA.

sample A can easily fly over to the p-GaN layer where they can recombine with holes radiatively or nonradiatively. Therefore, a large portion of holes are consumed in the p-type region without being injected into the MQWs, leading to the lowest hole concentration in the MQWs of sample A. When EBL is adopted in either sample B or C, the chance for leakage of electrons into the p-GaN layer is lower, and thus holes are less recombined with the leaked electrons and are more likely injected into MQWs, which leads to the generally higher hole concentrations in sample B and C than in sample A. In addition, the hole concentrations in the MQWs of sample C is significantly higher than that of sample B, which should be associated with the higher blocking barrier for electron leakage and the simultaneously lower barrier for hole injection resulting from Al content graded EBL in sample C as compared to the p-$Al_{0.7}Ga_{0.3}N$ EBL in sample B. The more effective electron blocking effect and lower barrier for hole injection together lead to the highest hole concentration in MQWs of sample C. We also notice that the hole concentration in the Al content graded EBL of sample C is much higher ($> 1 \times 10^{18}$ cm^{-3}) than that of the p-$Al_{0.7}Ga_{0.3}N$ EBL in sample B ($\sim 6 \times 10^{13}$ cm^{-3}), which is responsible for the much higher conductivity in the Al content graded EBL and the correspondingly much lower working voltage in sample C than in sample B. The high hole concentration in Al content graded EBL is thought to be originated from the polarization gradient due to the linearly varied Al composition from 0.9 to 0.4 along the growth direction. The polarization gradient generates a high density of negative polarization charges, for which a high density of holes is attracted to compensate.

The effects of different EBLs on the electron leakage are also manifested by the profiles of electron current densities for the three structures, as shown in Fig. 5. Electrons are injected from the n-type side into MQWs and recombine with holes transported from the p-type region, which leads to

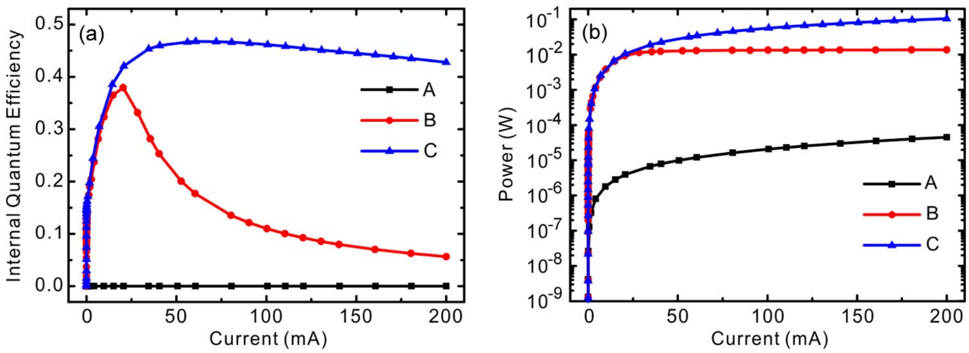

Fig. 6. Plots of (a) internal quantum efficiency and (b) light output power as functions of driving current for the three samples.

a lower electron current density in the p-type side than that in the n-type side. The electron current overflowing to the p-type layers is defined as the electron leakage current. As shown in Fig. 5, the ratio of the electron leakage current to the injection electron current is almost 100% in sample A, which means that most of the injected electrons in sample A escape out of the active region into the p-type GaN layer without contributing to wanted light emission. With the adoption of the p-$Al_{0.7}Ga_{0.3}N$ EBL in sample B, the ratio decreases to about 90%, indicating that although the electron leakage is somewhat reduced, it still remains dominant. When replacing the p-$Al_{0.7}Ga_{0.3}N$ EBL with Al content graded one the ratio becomes almost zero. Therefore, it can be concluded that the Al content graded EBL is much more effective in preventing electrons escaping from the active region into the p-GaN layer.

Fig. 6 shows the plots of IQE and light output power as functions of the injection current for the three samples. The IQE of sample A is extremely low at all current levels, which is obviously due to the severe electron leakage as described above. The almost 100% leakage of electrons into the p-GaN layer not only results in the very low electron concentrations in MQWs, but also depletes holes in the p-GaN so that hole concentrations are also very low in MQWs, both of which lead to the extremely low IQE in sample A. The issue of electron leakage in UV LEDs without EBL was also discussed in Ref. [32], where about 50% electron leakage was found. The less electron leakage in Ref. [32] could be mainly due to the usage of p-$Al_{0.6}Ga_{0.4}N$ cladding layer right after the $Al_{0.55}Ga_{0.45}N/Al_{0.49}Ga_{0.51}N$ MQWs, which might also block electrons even without the 1 nm AlN EBL. The IQEs of the other two samples with EBLs are obviously improved compared with sample A. The IQE of sample B reaches the maximum value of 37.9% at current of 20 mA, and then drops rapidly as the current increases (down to only 6% as the current rises to 200 mA). For sample C, when the current is below 15 mA, it has almost the same IQE as sample B. After the current exceeds 15 mA, the IQE of sample C still increases until the current reaches 60 mA, where its IQE has the maximum value of 46%. After that, the IQE of sample C slowly decreases, and reaches a value of 42% at the current of 200 mA. Therefore, sample C not only has higher maximum IQE but also has much lower efficiency droop as compared to sample B. As shown in Fig. 6(b), at the bias current of 200 mA, the output powers of three samples are 0.0451, 13.7, and 103.9 mW for sample A, B and C, respectively. All these results demonstrate that sample C has the best performance overall because of the largest maximum IQE value and lowest efficiency droop, which are all attributed to the great advantages of Al content graded EBL in providing effective electron blocking at the interface of the last barrier and EBL, and at the same time reducing barrier for hole injection at EBL/p-GaN interfaces.

4. Conclusion

In summary, we have investigated the effects of different EBLs on the performance of $Al_xGa_{1-x}N$ based 310 nm deep UV LEDs. The device structure without EBL suffers from the high electron leakage out of the active region into the p-type region, which results in very low IQEs at all injection currents due to the very low densities of electrons and holes in the MQWs. The adoption of EBL can effectively suppress the spill-over of electrons out of the active region, and thus can greatly improve the IQE. However, due to the high resistivity of the conventional $Al_{0.7}Ga_{0.3}N$ EBL, the working voltage is unacceptably high for the corresponding device structure. On the other hand, the Al content graded EBL has a much higher conductivity due to the presence of high concentration of holes, which results in reasonable working voltages. In addition, the Al content graded EBL has the great advantages of higher blocking barrier for electron leakage and the simultaneously lower barrier for hole injection, which results in much higher densities of electrons and holes in MQWs at high injection currents. Therefore, the adoption of Al content graded EBL in deep UV LEDs has great promise in improving the overall device performance.

Acknowledgment

The authors wish to thank the anonymous reviewers for their valuable suggestions.

References

[1] M. Shatalov, W. Sun, A. Lunev, X. Hu, A. Dobrinsky, Y. Bilenko, J. Yang, M. Shur, R. Gaska, C. Moe, G. Garrett, and M. Wraback, "AlGaN deep-ultraviolet light-emitting diodes with external quantum efficiency above 10%," *Appl. Phys. Exp.*, vol. 5, no. 8, pp. 082101-1–082101-3, Jul. 2012.
[2] C. Pernot, S. Fukahori, T. Inazu, T. Fujita, M. Kim, Y. Nagasawa, A. Hirano, M. Ippommatsu, M. Iwaya, S. Kamiyama, I. Akasaki, and H. Amano, "Development of high efficiency 255-355 nm AlGaN-based light-emitting diodes," *Phys. Stat. Sol. (A)*, vol. 208, no. 7, pp. 1594–1596, Jul. 2011.
[3] M. Kneissl, T. Kolbe, C. Chua, V. Kueller, N. Lobo, J. Stellmach, A. Knauer, H. Rodriguez, S. Einfeldt, Z. Yang, N. M. Johnson, and M. Weyers, "Advances in group III-nitride-based deep UV light-emitting diode technology," *Semicond. Sci. Technol.*, vol. 26, no. 1, pp. 014036-1–014036-6, Jan. 2011.
[4] Y. Narukawa, M. Sano, M. Ichikawa, S. Minato, T. Sakamoto, T. Yamada, and T. Mukai, "Improvement of luminous efficiency in white light emitting diodes by reducing a forward-bias voltage," *Jpn. J. Appl. Phys.*, vol. 46, no. 40, pp. L963–L965, Oct. 2007.
[5] A. Khan, K. Balakrishnan, and T. Katona, "Ultraviolet light-emitting diodes based on group three nitrides," *Nat. Photonics*, vol. 2, no. 2, pp. 77–84, Feb. 2008.
[6] K. X. Chen, Q. Dai, W. Lee, J. K. Kim, F. E. Schubert, J. Grandusky, M. Mendrick, X. Li, and J. A. Smart, "Effect of dislocation on electrical and optical properties of n-type $Al_{0.34}Ga_{0.66}N$," *Appl. Phys. Lett.*, vol. 93, no. 19, pp. 192108-1–192108-3, Nov. 2008.
[7] H. Hirayama, T. Yatabe, N. Noguchi, T. Ohashi, and N. Kamata, "231-261 nm AlGaN deep-ultraviolet light-emitting diodes fabricated on AlN multilayer buffers grown by ammonia pulse-flow method on sapphire," *Appl. Phys. Lett.*, vol. 91, no. 7, pp. 071901-1–071901-3, Aug. 2007.
[8] J. Piprek, C. Moe, S. Keller, S. Nakamura, and S. P. Denbaars, "Internal efficiency analysis of 280 nm light emitting diodes," in *Proc. SPIE*, 2004, vol. 5594, pp. 177–184.
[9] M.-F. Huang and T.-H. Lu, "Optimization of the active-layer structure for the deep-UV AlGaN light-emitting diodes," *IEEE J. Quantum Electron.*, vol. 42, no. 8, pp. 820–826, Aug. 2006.
[10] K. H. Kim, Z. Y. Fan, M. Khizar, M. L. Nakarmi, J. Y. Lin, and H. X. Jiang, "AlGaN-based ultraviolet light-emitting diodes grown on AlN epilayers," *Appl. Phys. Lett.*, vol. 85, no. 20, pp. 4777–4779, Nov. 2004.
[11] J. P. Zhang, X. Hu, Y. Bilenko, J. Deng, A. Lunev, M. S. Shur, R. Gaska, M. Shatalov, J. W. Yang, and M. A. Khan, "AlGaN-based 280 nm light-emitting diodes with continuous-wave power exceeding 1 mW at 25 mA," *Appl. Phys. Lett.*, vol. 85, no. 23, pp. 5532–5534, Dec. 2004.
[12] R. A. Arif, Y.-K. Ee, and N. Tansu, "Polarization engineering via staggered InGaN quantum wells for radiative efficiency enhancement of light emitting diodes," *Appl. Phys. Lett.*, vol. 91, no. 9, pp. 091110-1–091110-3, Aug. 2007.
[13] H. Zhao, G. Liu, J. Zhang, J. D. Poplawsky, V. Dierolf, and N. Tansu, "Approaches for high internal quantum efficiency green InGaN light-emitting diodes with large overlap quantum wells," *Opt. Exp.*, vol. 19, no. S4, pp. A991–A1007, Jul. 2011.
[14] H. Zhao, R. A. Arif, and N. Tansu, "Design analysis of staggered InGaN quantum wells light-emitting diodes at 500–540 nm," *IEEE J. Sel. Topics Quantum Electron.*, vol. 15, no. 4, pp. 1104–1114, Jul./Aug. 2009.
[15] H. P. Zhao, G. Y. Liu, X.-H. Li, R. A. Arif, G. S. Huang, J. D. Poplawsky, S. T. Penn, V. Dierolf, and N. Tansu, "Design and characteristics of staggered InGaN quantum-well light-emitting diodes in the green spectral regime," *IET Optoelectron.*, vol. 3, no. 6, pp. 283–295, Dec. 2009.
[16] C.-T. Liao, M.-C. Tsai, B.-T. Liou, S.-H. Yen, and Y.-K. Kuo, "Improvement in output power of a 460 nm InGaN light-emitting diode using staggered quantum well," *J. Appl. Phys.*, vol. 108, no. 6, pp. 063107-1–063107-6, Sep. 2010.
[17] S.-H. Park, D. Ahn, B.-H. Koo, and J.-W. Kim, "Dip-shaped InGaN/GaN quantum-well light-emitting diodes with high efficiency," *Appl. Phys. Lett.*, vol. 95, no. 6, pp. 063507-1–063507-3, Aug. 2009.
[18] R. A. Arif, H. Zhao, and N. Tansu, "Type-II InGaN-GaNAs quantum wells for lasers applications," *Appl. Phys. Lett.*, vol. 92, no. 1, pp. 011104-1–011104-3, Jan. 2008.
[19] H. Zhao, R. A. Arif, and N. Tansu, "Self-consistent gain analysis of type-II 'W' InGaN–GaNAs quantum well lasers," *J. Appl. Phys.*, vol. 104, no. 4, pp. 043104-1–043104-7, Aug. 2008.

[20] S.-H. Park, D. Ahn, B.-H. Koo, and J.-E. Oh, "Optical gain improvement in type-II InGaN/GaNSb/GaN quantum well structures composed of InGaN/and GaNSb layers," *Appl. Phys. Lett.*, vol. 96, no. 5, pp. 051106-1–051106-3, Feb. 2010.
[21] J. Park and Y. Kawakami, "Photoluminescence property of InGaN single quantum well with embedded AlGaN δ layer," *Appl. Phys. Lett.*, vol. 88, no. 20, pp. 202107-1–202107-3, May 2006.
[22] S.-H. Park, J. Park, and E. Yoon, "Optical gain in InGaN/GaN quantum well structures with embedded AlGaN δ layer," *Appl. Phys. Lett.*, vol. 90, no. 2, pp. 023508-1–023508-3, Jan. 2007.
[23] H. Zhao, G. Liu, and N. Tansu, "Analysis of InGaN-delta-InN quantum wells for light-emitting diodes," *Appl. Phys. Lett.*, vol. 97, no. 13, pp. 131114-1–131114-3, Sep. 2010.
[24] H. Zhao, G. Liu, R. A. Arif, and N. Tansu, "Current injection efficiency induced efficiency-droop in InGaN quantum well light-emitting diodes," *Solid-State Electron.*, vol. 54, no. 10, pp. 1119–1124, Oct. 2010.
[25] M. F. Schubert, J. Xu, J. K. Kim, E. F. Schubert, M. H. Kim, S. Yoon, S. M. Lee, C. Sone, T. Sakong, and Y. Park, "Polarization-matched GaInN/AlGaInN multi-quantum-well light-emitting diodes with reduced efficiency droop," *Appl. Phys. Lett.*, vol. 93, no. 4, pp. 041102-1–041102-3, Jul. 2008.
[26] N. F. Gardner, G. O. Muller, Y. C. Shen, G. Chen, S. Watanabe, W. Gotz, and M. R. Krames, "Blue-emitting InGaN-GaN double heterostructure light-emitting diodes reaching maximum quantum efficiency above 200A/cm^2," *Appl. Phys. Lett.*, vol. 91, no. 24, pp. 243506-1–243506-3, Dec. 2007.
[27] H. Hirayama, S. Fujikawa, N. Noguchi, J. Norimatsu, T. Takano, K. Tsubaki, and N. Kamata, "222-282 nm AlGaN and InAlGaN-based deep-UV LEDs fabricated on high-quality AlN on sapphire," *Phys. Stat. Sol. (A)*, vol. 206, no. 6, pp. 1176–1182, Jun. 2009.
[28] T. Nishida, H. Saito, and N. Kobayashi, "Milliwatt operation of AlGaN-based single-quantum-well light emitting diode in the ultraviolet region," *Appl. Phys. Lett.*, vol. 78, no. 25, pp. 3927–3928, Jun. 2001.
[29] R. Gutt, T. Passow, M. Kunzer, W. Pletschen, L. Kirste, K. Forghani, F. Scholz, K. Kohler, and J. Wagner, "AlGaN based 355 nm UV light-emitting diodes with high power efficiency," *Appl. Phys. Exp.*, vol. 5, no. 3, pp. 032101-1–032101-3, Feb. 2012.
[30] Y. Liao, C. Thomidis, C.-K. Kao, and T. D. Moustakas, "AlGaN based deep ultraviolet light emitting diodes with high internal quantum efficiency grown by molecular beam epitaxy," *Appl. Phys. Lett.*, vol. 98, no. 8, pp. 081110-1–081110-3, Feb. 2011.
[31] J. C. Zhang, Y. H. Zhu, T. Egawa, S. Sumiya, M. Miyoshi, and M. Tanaka, "Suppression of the subband parasitic peak by 1 nm i-AlN interlayer in AlGaN deep ultraviolet light-emitting diodes," *Appl. Phys. Lett.*, vol. 93, no. 13, pp. 131117-1–131117-3, Sep. 2008.
[32] J. Piprek and Z. M. Simon Li, "Sensitivity analysis of electron leakage in III-nitride light-emitting diodes," *Appl. Phys. Lett.*, vol. 102, no. 13, pp. 131103-1–131103-4, Apr. 2013.
[33] J. Zhang, H. Zhao, and N. Tansu, "Effect of crystal-field split-off hole and heavy-hole bands crossover on gain characteristics of high Al-content AlGaN quantum well lasers," *Appl. Phys. Lett.*, vol. 97, no. 11, pp. 111105-1–111105-3, Sep. 2010.
[34] T. M. Al tahtamouni, J. Y. Lin, and H. X. Jiang, "Optical polarization in c-plane Al-rich AlN/$Al_xGa_{1-x}N$ quantum wells," *Appl. Phys. Lett.*, vol. 101, no. 4, pp. 042103-1–042103-3, Jul. 2012.
[35] J. Zhang and N. Tansu, "Engineering of AlGaN-delta-GaN quantum-well gain media for mid- and deep-ultraviolet lasers," *IEEE Photon. J.*, vol. 5, no. 2, pp. 2600209-1–2600209-9, Apr. 2013.
[36] J. Zhang, H. Zhao, and N. Tansu, "Large optical gain AlGaN-delta-GaN quantum wells laser active regions in mid- and deep-ultraviolet spectral regimes," *Appl. Phys. Lett.*, vol. 98, no. 17, pp. 171111-1–171111-3, Apr. 2011.
[37] Y. Taniyasu and M. Kasu, "Polarization property of deep-ultraviolet light emission from C-plane AlN/GaN short-period superlattices," *Appl. Phys. Lett.*, vol. 99, no. 25, pp. 251112-1–251112-4, Dec. 2011.
[38] G. Sun, Y. J. Ding, G. Liu, G. S. Huang, H. Zhao, N. Tansu, and J. B. Khurgin, "Photoluminescence emission in deep ultraviolet region from GaN/AlN asymmetric-coupled quantum wells," *Appl. Phys. Lett.*, vol. 97, no. 2, pp. 021904-1–021904-3, Jul. 2010.
[39] I. Vurgaftman, J. R. Meyer, and L. R. Ram-Mohan, "Band parameters for III-V compound semiconductors and their alloys," *J. Appl. Phys.*, vol. 89, no. 11, pp. 5815–5875, Jun. 2001.
[40] J. Piprek and S. Li, "Electron leakage effects on GaN-based light-emitting diodes," *Opt. Quantum Electron.*, vol. 42, no. 2, pp. 89–95, Jan. 2010.
[41] V. Fiorentini, F. Bernardini, F. D. Sala, A. D. Carlo, and P. Lugli, "Effects of macroscopic polarization in III-V nitride multiple quantum wells," *Phys. Rev. B*, vol. 60, no. 12, pp. 8849–8858, Sep. 1999.
[42] C. M. Caughey and R. E. Thomas, "Carrier mobilities in silicon empirically related to doping and field," *Proc. IEEE*, vol. 55, no. 12, pp. 2192–2193, Dec. 1967.